Theoretical investigation of crystalline electric field influence on the magnetocaloric effect in the cubic praseodymium system $PrNi_2$

P. J. von Ranke* and W. S. Torres

Instituto de Física, Universidade do Estado do Rio de Janeiro UERJ, Rua São, Francisco Xavier, 524, 20550-013 Rio de Janeiro, RJ, Brazil

(Received 25 June 2021; revised 2 January 2022; accepted 15 February 2022; published 28 February 2022)

We report a theoretical investigation of the magnetocaloric effect in paramagnetic intermetallic $PrNi_2$. We choose this particular compound because it presents high cubic symmetry, and two sets of crystalline electrical field parameters were reported, allowing a systematic study. In one of these sets, the magnetic entropy increases upon applied magnetic field in the low temperature region ($T < 10$ K) for $H = 5$ T. This anomaly was investigated through a model Hamiltonian which includes the magnetic, exchange, and crystalline electric field interactions. The simulated curves of the temperature dependence of isothermal entropy variation and adiabatic temperature change present the inverse magnetocaloric effect, which is not expected for a paramagnetic system.

DOI: 10.1103/PhysRevB.105.085153

I. INTRODUCTION

The magnetocaloric effect (MCE) is the thermal response of a magnetic material, when submitted to an applied magnetic field change. This response is usually measured through ΔS_T and ΔT_{ad}, namely, the isothermal entropy and adiabatic temperature changes upon magnetic field variation, respectively [1]. The MCE depends on several conditions, e.g., the material temperature and the crystallographic direction of applied magnetic field. In general, the MCE intensity reaches higher values around the temperature of magnetic phase transition and for magnetic field changes applied along the easy magnetic direction. Research on the MCE creates an enabling environment for an optimum balance between applied and basic sciences. From the applied point of view, the main focus is concerned with using the MCE materials as a refrigerant body to work in a magnetic refrigerator which can save energy; it is also a green technology [2–4]. On the basic search side, the MCEs are strongly correlated with several physical properties, e.g., magnetic and structural phases transitions [5,6], magnetoresistivity [7,8], disorder at the rare-earth sites [9], degree of magnetic sample amorphization [10], crystalline and magnetic anisotropy [11,12], and so on.

In a crystal lattice the $(2J + l)$-fold ground state degeneracy of rare-earth magnetic ions can be partially removed due to the neighboring electrical charges, the so-called crystal electrical field interaction (CEF). The remaining degeneracy is determined by the symmetry of the CEF at the rare-earth site. The MCE of rare-earth intermetallic compounds depends on the CEF interaction, which can generate strong magnetic anisotropy and a nonlinear magnetic field dependence of the $(2J + 1)$ energy levels. The rotating magnetocaloric effect, where ΔS_T and ΔT_{ad} are calculated by changing the magnetic field direction (instead of its intensity, which is fixed), is directly related with the CEF anisotropy [13–15]. In the paramagnetic $PrNi_5$ compound, an anomalous magnetocaloric was predicted through the calculation of nonlinear dependence of magnetic energy levels, due to the hexagonal CEF interaction. This compound presents an inverse magnetocaloric effect ascribed to the crossing of CEF levels [16].

In this work, we investigate the influence of CEF interaction on the paramagnetic $PrNi_2$. This compound has certain important characteristics and simplicities that allow a systematic study, namely: (1) cubic symmetry, where only two parameters are necessary to describe the CEF interaction; (2) low and integer value ($J = 4$) of total angular momentum; (3) the fundamental ground state is a nonmagnetic Γ_3 double, so the onset of magnetization can only be induced by an exchange or magnetic field through transition admixtures with excited states; and (4) there are two possible sets of CEF parameters, determined through the inelastic neutron scattering experiment. The first set of CEF parameters ($W = -0.23$ meV, $x = -0.64$) [17] leads to the ground and first excited level scheme, Γ_3 and Γ_5, and the second one ($W = -0.18$ meV, $x = 0.58$) [18] leads to Γ_3 and Γ_4. These two CEF levels schemes lead to marked differences in magnetocaloric potentials ΔS_T and ΔT_{ad}. Our systematic study of the influence of CEF on the MCE goes beyond the $PrNi_2$ system; it has been extended to the entire allowed space of the x CEF parameter, through the use of the Lea, Leask, and Wolf (LLW) diagram [19].

II. THEORY

The paramagnetic $PrNi_2$ compound crystallizes in the Laves phase ($C15$ structure) in which the Pr^{3+} ions are localized in equivalent sites of cubic point symmetry, so we need only two CEF parameters [17,18]. In the molecular field approximation, the magnetic behaviors of $PrNi_2$ are described by the following Hamiltonian:

$$H = W\left[x\left(\frac{O_4}{F_4}\right) + (1 - |x|)\left(\frac{O_6}{F_6}\right)\right] - g\mu_B \sum_{k=x,y,z} [\lambda\langle J^k\rangle + H\cos\alpha_k]J^k. \quad (1)$$

The first term gives the crystalline electrical field interaction in Lea, Leask, and Wolf (LLW) notation [19], where W

*von.ranke@uol.com.br

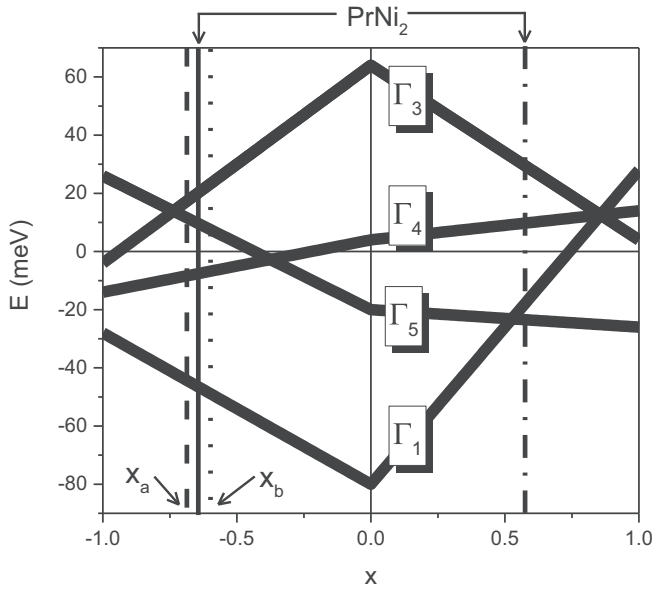

FIG. 1. LLW diagram showing the two investigated CEF level schemes for $PrNi_2$. Set 1 ($W = –0.23$ meV, $x = –0.64$): vertical solid line; set 2 ($W = –0.23$ meV, $x = –0.64$): vertical dash-dotted line.

scales the CEF energy levels splitting and x, $(-1 \leqslant x \leqslant 1)$ gives the ratio of fourth to sixth order terms of O_4 and O_6 operators. The $O_4 = O_4^0 + 5O_4^4$, $O_6 = O_6^0 - 21O_4^4$ are combinations of, O_n^m-Stevens's equivalent operators [20] and $F_4 = 60$, $F_6 = 1260$ are scale factors attributed to the Pr^{3+}. The second term represents the magnetic and exchange interactions, g being the Landé factor, μ_B the Bohr magneton, λ the exchange parameter, J^k the total angular momentum component, and $(H \to \mu_0 H)$ is the magnetic field applied along the cosine directions $(\cos\alpha_k)$.

Due to the CEF Hamiltonian in relation (1), the ninefold degenerate ground eigenvectors of the Pr^{3+} ion, written in J^z eigenvectors base, are decomposed into Γ_1 (singlet), Γ_3 (doublet), Γ_4 (triplet), and Γ_5 (triplet), given by

$$\Gamma_1 : |e_1\rangle = a|4\rangle + b|0\rangle + a|-4\rangle, \tag{2a}$$
$$\Gamma_3 : |e_2\rangle = c|4\rangle - d|0\rangle + c|-4\rangle, \tag{2b}$$
$$|e_3\rangle = e|2\rangle + e|-2\rangle, \tag{2c}$$
$$\Gamma_4 : |e_4\rangle = f|3\rangle + g|-1\rangle, \tag{2d}$$
$$|e_5\rangle = f|-3\rangle + g|1\rangle, \tag{2e}$$
$$|e_6\rangle = e|4\rangle - e|-4\rangle, \tag{2f}$$
$$\Gamma_5 : |e_7\rangle = g|3\rangle - f|-1\rangle, \tag{2g}$$
$$|e_8\rangle = g|-3\rangle - f|1\rangle, \tag{2h}$$
$$|e_9\rangle = e|2\rangle - e|-2\rangle. \tag{2i}$$

The coefficients, $a = \sqrt{30}/12$, $b = \sqrt{21}/6$, $c = \sqrt{42}/12$, $d = \sqrt{15}/6$, $e = \sqrt{2}/2$, $f = \sqrt{2}/4$ and $g = \sqrt{14}/4$, fix the orthonormality condition $\langle e_i|e_j\rangle = \delta_{ij}$ and do not depend on the x-CEF parameter. On the other hand, the CEF energy eigenvalues depend on the x-CEF parameter and can be mapped in the so-called LLW diagram, constructed with $W = 1$, as shown in Fig. 1 (thick lines).

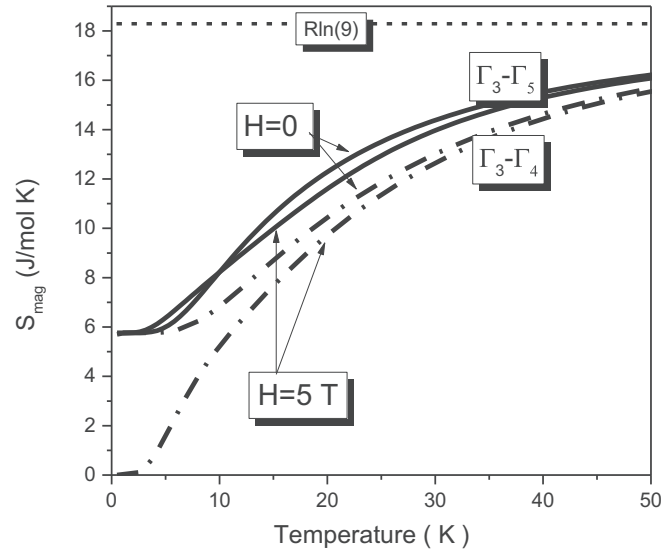

FIG. 2. Temperature dependence of magnetic entropy in $PrNi_2$, for $H = 0$ and 5 T, considering the two sets of parameters: Set 1 solid and set 2 dash-dotted curves.

The temperature and magnetic field dependence of the magnetic entropy are given by

$$S_{\rm mag}(T,H) = R\left[\sum_i \exp\left(-\frac{\varepsilon_i}{k_B T}\right) + \frac{1}{k_B T}\frac{\sum_i \varepsilon_i \exp\left(-\frac{\varepsilon_i}{k_B T}\right)}{\sum_i \exp\left(-\frac{\varepsilon_i}{k_B T}\right)}\right], \tag{3}$$

where R is the gas constant, k_B the Boltzmann constant, and ε_i the energy eigenvalues of the Hamiltonian given in relation (1).

III. RESULTS AND DISCUSSIONS

The two reported sets of CEF model parameters for $PrNi_2$ were used in this work: set 1: ($W = –0.23$ meV, $x = –0.64$) [17] and set 2: ($W = –0.18$ meV, $x = 0.58$) [18]. It is worth noticing that, in both sets $W < 0$; therefore, the LLW diagram should be read from top to bottom in the corresponding W scale (i.e., after multiplying the vertical axis of Fig. 1 by the respective value of W). In Fig. 1, the vertical solid ($x = –0.64$) and the dash-dotted ($x = 0.58$) lines indicate the CEF levels schemes, namely, set 1: Γ_3 (0), Γ_5 (2.539 meV), Γ_4 (6.440 meV), and Γ_1 (15.456 meV) and for set 2: Γ_3 (0), Γ_4 (3.492 meV), Γ_1 (8.381 meV), and Γ_5 (9.482 meV). These results were obtained with high precision, and set 1 is in good agreement with the ones in Ref. [17]. On the other hand, for set 2, a considerable discrepancy (of about 13%) was observed with the ones reported in Ref. [18]. For both sets of CEF parameters the easy magnetic direction is $\langle 001\rangle$ and the exchange parameter was taken from Ref. [17].

Figure 2 shows the temperature dependence of the magnetic entropy for the two sets of CEF parameters with and without applied magnetic field. For set 1, in which the ground and first excited states are $\Gamma_3 - \Gamma_5$, a crossing between the entropy curves for $H = 0$ and $H = 5$ T is observed around

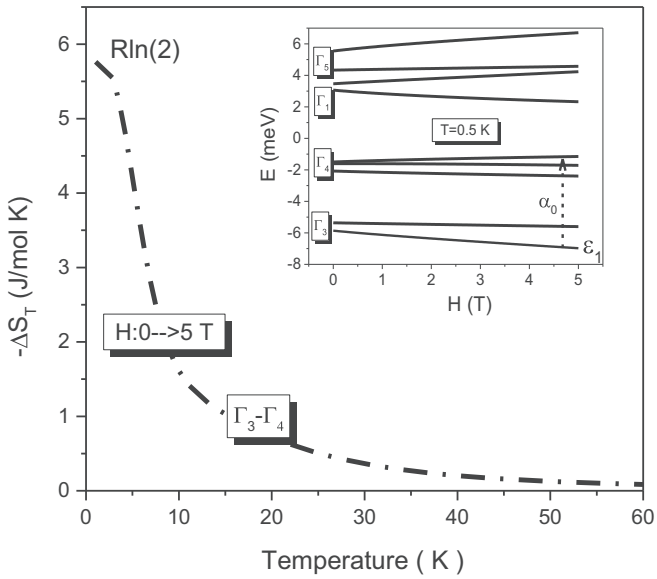

FIG. 3. Temperature dependence of $-\Delta S_T$ in $PrNi_2$, for magnetic field change from $H = 0$ to 5 T, using the parameters of set 2. The inset shows the energy level splitting due to the applied magnetic field.

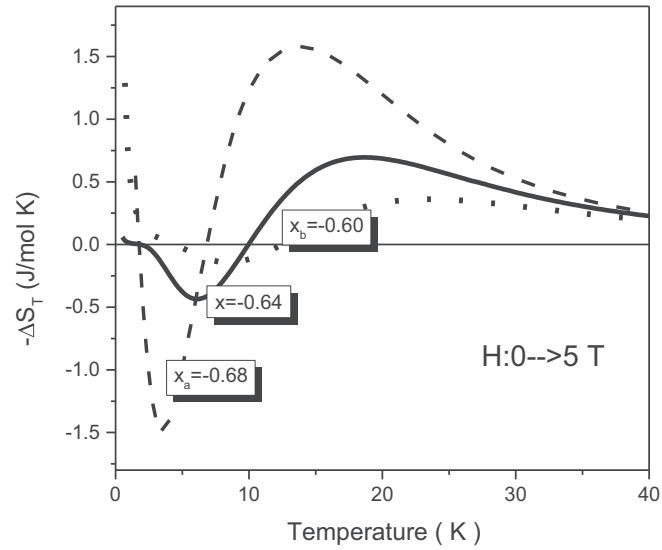

FIG. 4. Temperature dependence of $-\Delta S_T$ in $PrNi_2$, for magnetic field change from $H = 0$ to 5 T, using the parameters of set 1: solid curve. The dashed and dotted curves were calculated using the x-CEF parameters $x_a = -0.68$ and $x_b = -0.60$, respectively, as displayed in the LLW diagram.

$T = 10\,\mathrm{K}$. Below $T = 10\,\mathrm{K}$, an anomalous effect occurs in which the magnetic entropy increases when the magnetic field is applied. Above $T = 10\,\mathrm{K}$, the magnetic entropy decreases with increasing magnetic field and saturates at $S_{\mathrm{mag}}(\mathrm{max}) = R\ln(9)$, where R is the gas constant, as expected. As the temperature goes to zero, in zero field, we obtain $S_{\mathrm{mag}}(\mathrm{min}) = R\ln(2)$, which is ascribed to the doublet ground state. For set 2, in which the ground and first excited states are $\Gamma_3 - \Gamma_4$, the magnetic entropy decreases with magnetic field in the entire temperature range. For $H = 5\,\mathrm{T}$, and temperature above $T = 0.5\,\mathrm{K}$, the Γ_3 doublet splits into two singlet states so the magnetic entropy goes to zero for the low temperature region, as shown in the dash-dotted curve for $H = 5\,\mathrm{T}$.

Figure 3 shows the temperature dependence of isothermal entropy change $\Delta S_T = S_{\mathrm{mag}}(T, H = 5\,\mathrm{T}) - S_{\mathrm{mag}}(T, H = 0)$, considering set 2 of CEF parameters. The maximum value of $\Delta S_T = R\ln(2)$ is achieved as $T \to 0\,\mathrm{K}$. The inset shows the splitting of the nine energy levels [see relation (2)] as the magnetic field increases from zero to five T, at $T = 0.5\,\mathrm{K}$. The strong magnetic field dependence of the fundamental energy level $\varepsilon_1(H)$ comes from the allowed transition $\alpha_0 = \langle e_6|J^z|e_2\rangle = \langle e_2|J^z|e_6\rangle = \sqrt{84}/3$, which admixtures the nonmagnetic ground state $|e_2\rangle$ with the $|e_6\rangle$ (see the dotted arrow) [21].

Figure 4 shows the temperature dependence of ΔS_T, upon magnetic field variation from 0 to 5 T, for set 1 (solid curve). Using set 1, an inverse magnetocaloric effect (defined as $-\Delta S_T < 0$) was predicted in the calculated temperature interval from $T = 0.5\,\mathrm{K}$ to $T \sim 10\,\mathrm{K}$. The inverse magnetocaloric effect is not expected in a paramagnetic system as is the case for $PrNi_2$. A systematic analysis was performed considering a small change in the x-CEF parameter around the fixed value of set 1 ($x = -0.64$). The dotted and dashed curves in Fig. 4 show ΔS_T vs T for $x_a = -0.68$ and $x_b = -0.6$, respectively, for the same W scale used in set 1. The vertical dashed and dotted lines for x_a and x_b are displayed in the LLW diagram (Fig. 1) and preserve the same order of CEF levels scheme ($\Gamma_3 - \Gamma_5 - \Gamma_4 - \Gamma_1$) from set 1. The intensity of anomalous minimum values in $-\Delta S_T$ vs T, namely: 0.14, 0.42 and $1.5\,\mathrm{J\,mol^{-1}\,K^{-1}}$, increases as the x CEF parameter approaches the crossing in energy levels ($\Gamma_3 - \Gamma_5$) (see the LLW diagram). In order to investigate the origin of this anomalous effect, which appears using the parameters of set 1, we plotted the magnetic field dependence of the nine energy states at $T = 0.5\,\mathrm{K}$, as shown in Fig. 5. Comparing

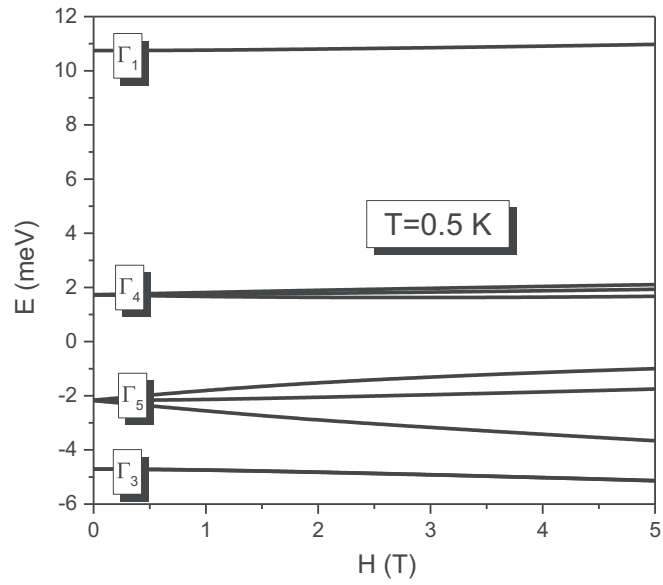

FIG. 5. Energy level splitting, due to the applied magnetic field with model parameters from set 1, at $T = 0.5\,\mathrm{K}$.

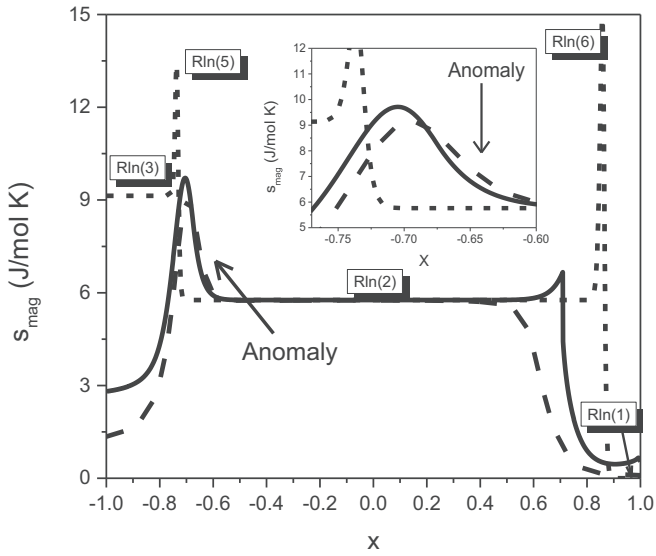

FIG. 6. Magnetic entropy versus x-CEF parameter, at $T = 1$ K. Dotted, solid, and dashed curves were obtained using, respectively: only CEF interaction, CEF plus exchange interaction, and CEF plus exchange and Zeeman interactions (with $H = 5$ T).

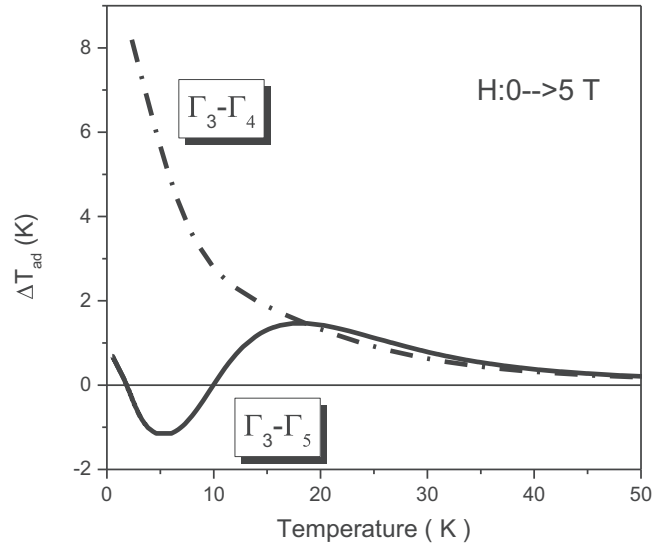

FIG. 7. Temperature dependence of ΔT_{ad} in $PrNi_2$, for magnetic field change from $H = 0$ to 5 T, using the parameters of set 1 (solid curve) and set 2 (dash-dotted curve).

these energy level splittings with the ones for set 2 (inset of Fig. 3), three striking differences and characteristics should be highlighted: (1) the admixtures of nonmagnetic ground state level Γ_3 with the exited magnetic ones can be neglected; i.e., the magnetic field practically does not change the energy of the fundamental level; (2) the double degeneracy, in the fundamental level, is kept for low values of the magnetic field; and (3) increasing the magnetic field, the first excited state approaches energetically to the ground state. Characteristics (1) and (2) lead to the observed value $R\ln(2)$ for the minimum entropy for ($T \to 0$ K) as show by the solid curve in Fig. 2 at $H = 5$ T. Characteristic (3) leads to anomalies in which the magnetic entropy increases when the magnetic field increases. In general, increasing the magnetic field separates the magnetic energy levels (Zeeman effect), decreasing the density of states, and consequently decreasing the entropy. On the other hand, if the energy levels approach with increasing magnetic field (increasing the density of states), the entropy increases.

To show that the region around $x = -0.64$, where the anomaly appears, is singular in the entire interval ($-1 < x < 1$), we studied the x-CEF parameter dependence of magnetic entropy. As shown in Fig. 6, calculations were performed with $W = -0.23$ meV of set 1, at $T = 1$ K, in three scenarios: (I) only CEF interaction, represented by the dotted curve; (II) CEF plus exchange interaction, represented by the solid curve;and (III) CEF plus exchange and Zeeman interactions (with $H = 5$ T), represented by the dashed curve. In scenario (I), the plateau in the interval ($-1 < x < -0.75$) describes the entropy value $R\ln(3)$ due to the Γ_5 (triplet), ground state. The entropy peaks at $x = -0.74$ achieving the value of $R\ln(5)$ due to the crossing between Γ_5 (triplet) and Γ_3 (doublet), as shown in the LLW diagram (Fig. 1). The long plateau, from $x = -0.73$ to 0.83, has the value $R\ln(2)$, since in this region Γ_3 (doublet) is the ground state. Around $x = 0.85$ a high peak of $R\ln(6)$ appears due to the crossing among Γ_3 (doublet), Γ_4 (triplet), and Γ_1 (singlet). From $x = 0.88$ to 1, the magnetic entropy vanishes since in this interval the ground state is Γ_1 (singlet). In scenario (II), where the exchange interaction is included, the two peaks observed in scenario (I) decrease and approach each other. Furthermore, the central plateau regions are reduced. In scenario (III), when the magnetic field is included, the left peak is displaced to high x values and the right peak disappears. Therefore, comparing the curves of magnetic entropy with $H = 0$ and $H = 5$ T, solid and dashed curves in Fig. 6, we can conclude that only around $x = -0.64$ (see the arrow) does the magnetic entropy increase with magnetic field. The inset in Fig. 6 magnifies the narrow and singular region of the x-CEF parameter, where the anomaly appears.

In order to obtain the adiabatic temperature change, ΔT_{ad}, upon magnetic field change in $PrNi_2$, the lattice and electronic entropy must be added [1]. At low temperature, the electronic entropy is given by $S_{el} = \gamma T$ and the lattice entropy $S_{\text{latt}} = S_{\text{latt}}(\Theta_D, T)$, was taken in the Debye assumptions. The parameters γ (Sommerfeld parameter) and Θ_D (Debye temperature) for $PrNi_2$ were taken from the heat capacity measurement in $LaNi_2$ (an isostructural, nonmagnetic compound), namely: $\gamma = 12.52$ mJ mol^{-1} K^{-2} and $\Theta_D = 242$ K [22]. Figure 7 shows the temperature dependence of the adiabatic temperature change in $PrNi_2$, for magnetic field variation from $H = 0$ to $H = 5$ T. The solid and dashed curves were calculated using the CEF parameters from set 1 and set 2, respectively. As expected, set 2 leads to normal magnetocaloric effect. For set 1, an anomalous magnetocaloric effect is predicted in which the *paramagnetic compound* $PrNi_2$ *cools down upon magnetic field application* below $T \sim 10$ K, for magnetic field change from $H = 0$ to 5 T. The above calculation was performed upon magnetic field change from $H = 0$ to 5 T; the calculations for lower magnetic field changes, e.g., $H = 0$ to 2 T show the same profile, reducing only the peak intensity values.

IV. FINAL COMMENTS

A striking and conceptual characteristic of a paramagnetic system consists of decreasing magnetic entropy when a magnetic field is applied. This behavior is expected due to the alignment of the magnetic moments along the field direction. Using a microscopic model, we predicted an anomalous magnetocaloric effect in a simple cubic paramagnetic compound $PrNi_2$, for set 1 ($W = -0.23$ meV, $x = -0.64$) CEF parameters. This anomaly leads our investigated paramagnetic system to cooling down (in an adiabatic process) and increasing magnetic entropy (in an isothermal process) upon magnetic field application, at low temperature ($T < 10$ K). This anomalous effect comes from the unusual CEF splinting of the $(2J + 1)$ fundamental multiplet of Pr^{3+} ($J = 4$) in the $PrNi_2$ compound. The nonmagnetic doublet Γ_3 ground state is almost independent of magnetic field due to the weak admixtures with the excited magnetic levels and the first excited level converges to doublet Γ_3, when the magnetic field increases. This behavior is opposite to what is observed in the usual Zeeman effect for a paramagnetic system, where the energy levels $\epsilon_m \propto mH$, $(m = J, J-1, \cdots, -J)$ diverge linearly when the magnetic field increases, which leads to increasing entropy.

To confirm our theoretical prediction, experimental results are desired, preferably in a monocrystalline sample, where the anomalous magnetocaloric effect in $PrNi_2$ should be more prominent than in a polycrystalline sample, as discussed in Ref. [16].

ACKNOWLEDGMENTS

We acknowledge financial support from CNPq–Conselho Nacional de Desenvolvimento Científico e Tecnológico.

P.J.v.R. conceived the study and wrote the manuscript. W.S.T. discussed and performed the theoretical calculations.

The authors declare that they have no known competing financial interests or personal relationships that could have appeared to influence the work reported in this paper.

[1] N. A. de Oliveira and P. J. von Ranke, Phys. Rep. **489**, 89 (2010).
[2] K. A. Gschneidner, Jr., V. K. Pecharsky, and A. O. Tsokol, Rep. Prog. Phys. **68**, 1479 (2005).
[3] V. Franco, J. S. Blázquez, J. J. Ipus, J. Y. Law, L. M. Moreno-Ramírez, and A. Conde, Prog Mater. Sci. **93**, 112 (2018).
[4] N. A. Zarkevich and V. I. Zverev, Crystals **10**, 815 (2020).
[5] C. Fang, G. Li, J. Wang, W. D. Hutchison, Q. Y. Ren, Z. Deng, G. Ma, S. Dou, S. J. Campbell, and Z. Cheng, Sci. Rep. **7**, 45814 (2017).
[6] S. Ghosh and S. Ghosh, Phys. Rev. B **103**, 054101 (2021).
[7] J. C. P. Campoy, E. J. R. Plaza, A. A. Coelho, and S. Gama, Phys. Rev. B **74**, 134410 (2006).
[8] P. J. von Ranke, P. O. Ribeiro, A. Magnus G. Carvalho, B. P. Alho, T. S. T. Alvarenga, E. P. Nobrega, A. Caldas, V. S. R. de Sousa, P. H. O. Lopes, and N. A. de Oliveira, J. Appl. Phys. **119**, 183903 (2016).
[9] E. P. Nobrega, N. A. de Oliveira, P. J. von Ranke, and A. Troper, Phys. Rev. B **74**, 144429 (2006).
[10] P. J. von Ranke, E. P. Nóbrega, A. Caldas, B. P. Alho, P. O. Ribeiro, T. S. T. Alvarenga, P. H. O. Lopes, V. S. R. de Sousa, A. Magnus, G. Carvalho, and N. A. de Oliveira, J. Magn. Magn. Matter. **369**, 34 (2014).
[11] P. J. von Ranke, N. A. de Oliveira, E. J. R. Plaza, V. S. R. de Sousa, B. P. Alho, A. Magnus, G. Carvalho, S. Gama, and M. S. Reis, J. Appl. Phys. **104**, 093906 (2008).
[12] N. A. de Oliveira and J. Caro Patiño, J. Appl. Phys. **127**, 125108 (2020).
[13] S. A. Nikitin, K. P. Skokov, Y. S. Koshkid'ko, Y. G. Pastushenkov, and T. I. Ivanova, Phys. Rev. Lett. **105**, 137205 (2010).
[14] J. C. B. Monteiro and F. G. Gandra, J. Appl. Phys. **121**, 213904 (2017).
[15] M. Orendáč, S. Gabáni, E. Gažo, G. Pristáš, N. Shitsevalova, K. Siemensmeyer, and K. Flachbart, J. Magn. Magn. Mater. **482**, 186 (2019).
[16] P. J. von Ranke, V. K. Pecharsky, K. A. Gschneidner, Jr., and B. J. Korte, Phys. Rev. B **58**, 14436 (1998).
[17] A. Andreeff, Th. Frauenheim, E. A. Goremychkin, H. Griessmann, B. Lippold, W. Matz, O. D. Chistyarov, and E. M. Savitskii, Phys. Status Solidi B **111**, 507 (1982).
[18] E. A. Goremychkin, I. Natkaniec, E. Mühle, and O. D. Chistyakov, J. Magn. Magn. Matter. **81**, 63 (1989).
[19] K. Lea, M. Leask, and W. Wolf, J. Phys. Chem. Solids **23**, 1382 (1962).
[20] K. W. H. Stevens, Proc. Phys. Soc. A **65**, 209 (1952).
[21] A. Caldas, P. J. von Ranke, and L. Palermo, Phys. Status Solidi B **175**, 497 (1993).
[22] H. H. Neumann, S. Nasu, R. S. Craig, N. Marzouk, and W. E. Wallace, J. Phys. Chem. Solids **32**, 2788 (1971).